# MACS-HAP: DESIGN AND IMAGE PROCESSING FEATURES OF THE DLR HAP CAMERA SYSTEM

*Joerg Brauchle[1], Veronika Gstaiger[2], Seyedmajid Azimi[2], Manuel Muehlhaus[2], Florian Nikodem[3], Patrick Dern[1], Derek Griffith[1]*

German Aerospace Center (DLR)
[1] Institute of Optical Sensor Systems, Berlin, Germany
[2] Remote Sensing Technology Institute, Oberpfaffenhofen, Germany
[3] Institute of Flight Systems, Brunswick, Germany
Email: [firstname.lastname]@DLR.de

## ABSTRACT

Recent developments in the construction and operation of high-altitude platforms (HAPs) close the gap between airborne and spaceborne remote sensing. The possibility of permanent monitoring of regions from the stratosphere offers new fields of application requiring bespoke instruments for operation on HAP carriers.

The *MACS-HAP* aerial camera system was developed specifically for platforms operating in the stratosphere. Based on a refractive optical design, it captures aerial images with 127 megapixels per image and achieves a ground sampling distance of 15 cm per pixel at 20 km altitude. One of the special system features is the embedded onboard processing hardware with specific algorithms for real-time information extraction.

This paper presents an overview of the instrument and the current state of development. Technical solutions to meet the specific payload requirements are described, such as stress-optimized design and the lightweight optical system with its capabilities for automatic onboard image processing.

***Index Terms***— High Altitude Platform, MACS-HAP, Aerial Camera, Stratosphere Remote Sensing, Image Processing, Deep Learning

## 1. INTRODUCTION

The use of HAPs as alternative carriers for communication and observation systems is becoming increasingly important as they are able to remain stationary over a certain region. These aircrafts operate in the rarely populated altitude band between 15 and 22 km and offer a cost-effective potential alternative to satellites. Research on such platforms is not only focused on design, solar generators or airspace integration. Together with new technologies, like artificial intelligence, the performance of HAP-payload-systems is increased and further fields of application are opened up, particularly in environmental research, disaster management or maritime surveillance [1][2].

The DLR currently develops the heavier-than-air platform *HAP alpha* to be operated in the stratosphere [1][3][4]. The aircraft has a maximum take-off weight of 134 kg and a wingspan of 27 m. In 2024 the demonstrator will be integrated to a fully functional research aircraft and a corresponding ground segment. In parallel, two remote sensing systems are developed. One of the new instruments is the synthetic aperture radar HAPSAR [5]. The other payload is the Modular Aerial Camera System MACS-HAP as shown in Fig. 1 and Fig. 2

## 2. MACS-HAP OPTICAL PAYLOAD

Optical remote sensing from the stratosphere provides unusual capabilities such as persistent monitoring of wide areas over weeks or months. This requires an aerial camera payload which is able to point independently from the platform. With the given optical design (see 2.1) an angular range of +/-30 deg off-nadir around roll and pitch axes covers a ground area of approximately 415 km² beneath the aircraft.

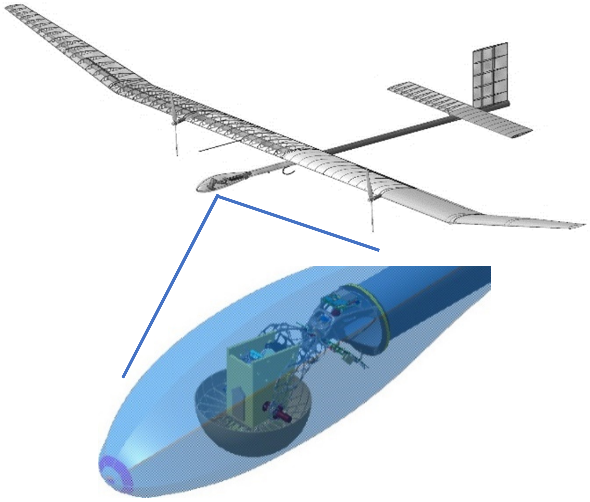

**Fig. 1:** Aerial camera system in payload compartment attached to front of *HAP alpha* fuselage; illustration.

However, operation on a solar powered aircraft results in limitations particularly regarding weight, power consumption and downlink data rate. Minimizing these aspects is necessary to achieve 24-hour cycles remaining above approximately 15 km where airspace population is rare enough. The instrument has a weight budget of 5 kg including all required parts, e.g. optical device, active gimbal, computers and the georeference / time system. The dimensions are 0.7 x 0.4 x 0.4 m³ (LxWxH). The payload setup is shown in Fig. 3. A hole in the compartment fairing leaves room for the lens to protrude and to rotate. For aerodynamic purposes, the half sphere closes the gap between lens and rim of the fairing's hole. An example for stress-optimized lightweight structure is shown in Fig. 3. Compared to a welded structure the weight was reduced by approximately 20% resulting in a cantilever weight of 230 g.

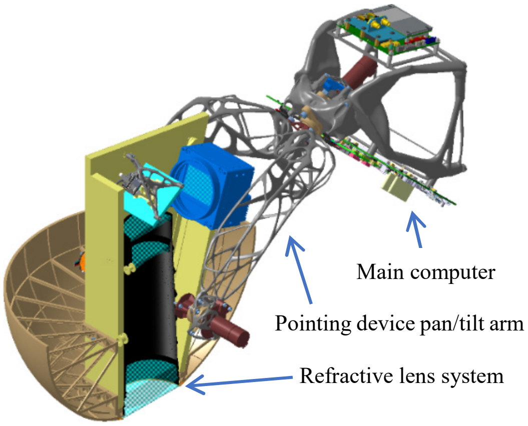

**Fig. 2:** MACS-HAP aerial camera assembly, partly sliced for illustration.

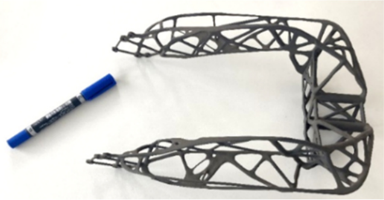

**Fig. 3:** Stress-optimized aluminum part: pan/tilt arm weighing 230 g.

### 2.1. Optical Design

Images are captured through a self-developed refractive lens system. Compared to a mirror design like a Three-Mirror Anastigmat (TMA), a glass design can be more compact reducing moments of inertia and thus minimizing the weight of the pointing device. The effort to seal a TMA against dust when landing and to fill the fairing gap was predicted as too high. The system is made for operation in the free atmosphere. However, glass lenses are sensitive against pressure and temperature changes, resulting in small image quality degradation. Regarding pressure, the design is calculated for 28 hPa. The pressure variation during daytime in the altitude band from 18 to 22 km is acceptable. The aforementioned strict mass limits do not leave room for an encapsulated and thermally conditioned enclosure making high temperature gradients the most critical risk to fracture one or more of the brittle lenses (see 2.2). The optical system properties are summarized in Table 1.

**Table 1:** Parameters of the optical system.

| | |
|---|---|
| Ground sampling distance | 15 cm @ 20 km alt. |
| Focal length | 500 mm |
| Aperture | 90 mm diameter |
| # of pixels per image | 127 Mpix (13392 x 9528) |
| Pixel pitch / iFOV | 3.76 µm / 7.5 µrad |
| Spectral band | RGB or NIR or PAN |
| Spectrum VNIR | ~450-900 nm |

The performance of the design represented by the Modulation Transfer Function (MTF) is shown in Fig. 4. This chart provides the quality of the image contrast depending on the object size. Details of 15 cm ground sampling distance correspond to 133 cycles (line pairs) per millimeter (3.76 µm sensor pixel pitch for which the lens was designed). Details of 15 cm size are resolved with a contrast of 0.27 or 27% in outer areas of the image (TS 3.8000 deg line meaning 3.8 deg from center line) and thus will be clearly distinguishable. The image center (TS 0.000 deg line) has a contrast of 0.3 showing that the degradation from center to the image edge is 3% and thus negligible.

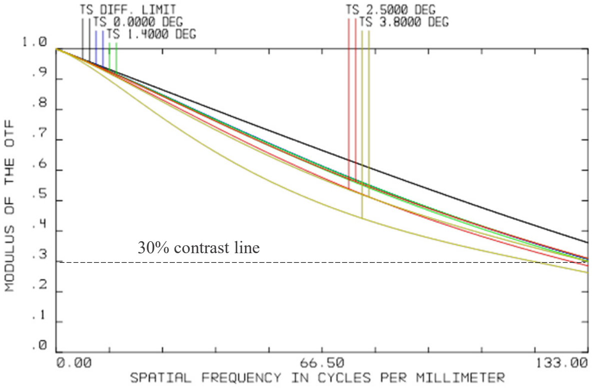

**Fig. 4:** Calculated MTF of the lens system.

A fold mirror reduces both assembly height and moments of inertia. The mirror can be moved translationally in 1.25 µm steps to compensate for temperature changes causing relevant focus shift. Images are captured by an industrial camera equipped with a global shutter CMOS sensor to avoid geometrical image distortion by camera movement during exposure. The optical path is shown in Fig. 5. In a future version the active gimbal will be used to compensate angular and translational aircraft motion in realtime. This enables the operation of a rolling shutter sensor. Such sensors provide higher dynamic range compared to global shutter sensors.

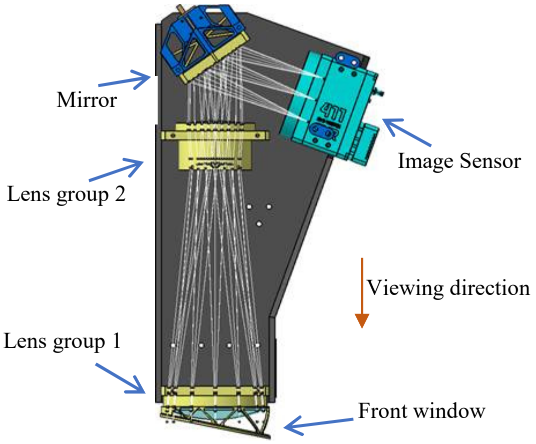

**Fig. 5:** Optical path, alignment of components; illustration.

## 2.2. Thermal design

One of the most critical engineering aspects is the thermal management of the payload. If forced convection would be used, the thin air at this altitude requires large fan diameters to generate sufficient air flow. Large heat spreaders matching such fans would imply a lot of additional mass. This was not acceptable since other components performance parameters would be impacted by mass budget transfer from these components to the heat spreaders. For this reason, the devices are cooled primarily by radiation. Black anodized aluminum plates attached directly on the heat source radiate to the environment. Heat-producing devices are arranged to avoid reflecting the emissions back or to heat adjacent components, seen in the right half of Fig. 2. Thermal straps are used to transfer heat to cold components, e.g. the stress-optimized structure holding the main computer. This structure is made of blackened 3D-printed aluminum.

Self-heating components, like image sensor, main computer, pointing unit controller and georeferencing system, have to be protected from overheating by reducing energy consumption and dissipating heat. The lenses must not be impacted by higher temperature gradients to maintain the optical performance and avoid lens fracture. Therefore, heat mats are applied within the case carrying the optical system. They are temporarily activated when the temperature in the cage drops below +10 °C.

The payload was simulated consuming 70 W for the daytime operation plus optional 2x 30 W to heat the case. Formulas used for the simulation are shown in [6][7][8]. Although the simulation in the literature is presented for the thermal analysis of wing sections, the payload simulation is based on the same formulas and assumptions. Dimensions of the payload compartment are 1.1 x 0.5 x 0.5 m³. It is covered with a technical fabric with assumed material properties $\lambda=0.25$, $\alpha=0.3$ and $\varepsilon=0.85$. The calculation shown in Table 2 was conducted for Kiruna during summer assuming the payload as one single box. Relevant altitudes are 20 km during daytime and 15 km at night. The temperatures are within the accepted range from -30 °C to +50 °C. One challenge is to distribute the heat away from hot spots like the main computer CPU and the image sensor by using weight-optimized radiation plates. The device-specific thermal simulations are in progress.

**Table 2:** Thermal simulation (preliminary result), relevant altitudes are 20 km by day and 15 km nights.

| Alt [km] | Air Density [kg/m³] | Day 100W [°C] | Night 30W [°C] | Night 130W [°C] |
|---|---|---|---|---|
| 0 | 1.3 | 24.9 | 9.3 | 13.4 |
| 5 | 0.7 | 9.5 | -11.0 | -6.1 |
| 10 | 0.4 | -3.7 | -27.4 | -21.4 |
| 15 | 0.2 | 2.7 | *{-19.9}* | *{-13.3}* |
| 20 | 0.1 | *{9.6}* | -11.0 | -4.0 |
| 25 | 0.04 | 17.4 | -1.2 | 6.1 |

## 2.3. Image Processing and Analysis

Acquired images are fed into an embedded PC where the onboard preprocessing is executed on-line. At this point there are two modes for further processing of the data.

Preferably, the georeferenced images are seamlessly cropped [9], lossy compressed and forwarded to the ground station via the 100 Mbit/s X-band radio downlink. In this operation mode, a particular region of interest is transmitted as frequently updated image mosaic which can be the basis for a dynamic situational map. Deep learning-based image enhancement and interpretation is executed in the ground station where work is being done to keep pace with the downlink data rates in order to perform further and more computationally intensive evaluations for potential real-time applications. Due to the flight altitude, atmospheric influences such as clouds or haze are to be expected. In order to increase the image quality, specific image enhancement is therefore developed and implemented [10]. This improves the quality of subsequent image evaluations, such as automated ship detection shown in Fig. 6 which was executed using ReDet [11]. Since there are further areas of application in the field of road traffic, powerful evaluation procedures for traffic research are also to be implemented at the ground station. Trained with DLR's EAGLE data set, one aim is to detect and classify vehicles quickly and validly [12]. The data can be used in models and simulations for mobility applications such as the management of connected vehicles or to support the operations of authorities and organizations with security tasks, for example in the event of natural disasters.

As the radio link data throughput decreases rapidly with a larger operational radius, additional onboard image processing is implemented. This mode uses extended AI-based real-time processing techniques running on a dedicated low power AI hardware device. Image enhancement as described above is performed to support subsequent evaluation algorithms [13] onboard and in real-time. In this case, the narrowband 500 kBit/s aircraft command and control link is used to transmit only the classification results or images of well-selected smaller regions for further analysis on the ground.

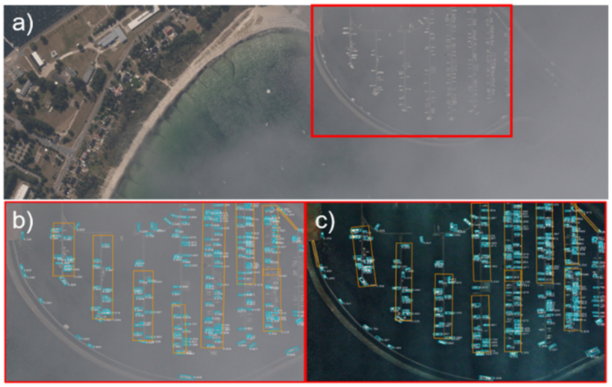

**Fig. 6:** Hazy aerial image (a) with automated ship (blue) and pier (orange) detection before (b) and after automated image enhancement (c).

## 3. OUTLOOK

The *MACS-HAP* optical sensor system including the components for further data processing and deployment offers ideal conditions for HAP-specific research and applications. A particular challenge is posed by the physical and environmental framework conditions for the system to realize wide area high-resolution image capturing with subsequent efficient image processing. While subsystems are already working laboratory setups, next steps are the critical design review, the MTF-measurement of the actual lens system and thermal flow simulation to dimension the cooling plates. Subsequently, the payload will be assembled and tested in the TVAC chamber. The first flight is planned for summer 2024.

In parallel, the image processing algorithms are enhanced to increase the analysis quality while further reducing the consumed energy and thus the heat impact. The goal is to enable the system to process 127 megapixel per second meaning one full image per second. The algorithms must keep up with the continuous image acquisition and data link throughput and still deliver valid results.

## 4. REFERENCES

[1] F. Nikodem, Florian and S. Kaltenhäuser, “Operation and operation approval of high-altitude platforms”, CEAS Aeronautical Journal (3). Springer. doi: 10.1007/s13272-020-00464-9, 2020.

[2] J. Brauchle, R. Berger, T. Hiebert and D. Hein “Towards Optical Maritime Surveillance with High-Altitude Platforms”, in Zenodo. European Workshop on Maritime Systems Resilience and Security (MARESEC 2021), 14. June 2021, Bremerhaven, Germany, 2021. https://zenodo.org/record/5604367#.Y8F4W3bMJaQ

[3] A. Voß, V. Handojo, C. Weiser and S. Niemann, Steffen, “Results from Loads and Aeroelastic Analyses of a High Altitude, Long Endurance, Solar Electric Aircraft”, in Journal of Aeroelasticity and Structural Dynamics, 9 (1), Department of Aerospace Engineering of Politecnico di Milano, pp. 1-22, 2022.

[4] S. Niemann, T. Gesell, S. Froese, M. Schollerer, M. Hanke, J. Nickel and A. Bärschneider, „Klebeverbindungen der Primärstruktur innerhalb des HAP-Projektes“, Deutscher Raumfahrtkongress (DLRK) 2021, 31. Aug. - 02. Sep. 2021, Bremen, Germany, 2021.

[5] M. Jirousek, M. Peichl, S. Anger, M. Engel, S. Dill, R. Scheiber and S. Baumgartner, ”Synthetic Aperture Radar Design for a High-Altitude Platform”, European Conference on Synthetic Aperture Radar, 2022-07-25 - 2022-07-27, Leipzig, Germany, 2022.

[6] O. C. Beneitez, “Thermal Management of Electrical Systems in a Solar-Electric Stratosphere HALE”, AIAA Aviation Forum 2022, 27 June - 01 July, Chicago, USA, 2022.

[7] Beneitez Ortega, Cristina und Zimmer, Dirk und Weber, Patrick (2023) *Thermal Analysis of a High-Altitude Solar Platform.* CEAS Aeronautical Journal. Springer. doi: 10.1007/s13272-022-00636-9. ISSN 1869-5590.

[8] Beneitez Ortega, Cristina und Zimmer, Dirk und Weber, Patrick (2021) *Thermal Management Concept Evaluation for a High-Altitude Solar Platform.* Lecture for the Aerospace Europe Conference 2021 submitted to the CEAS Journal, 23-26 Nov 2021, Warsaw, Poland.

[9] D. Hein and R. Berger “Terrain Aware Image Clipping for Real-Time Aerial Mapping”, in ISPRS Annals of the Photogrammetry, Remote Sensing and Spatial Information Sciences, IV (1), Copernicus Publications. ISPRS TC I Midtermn Symposium - Innovative Sensing - From Sensors to Methods and Applications, 9. Oct. - 12. Oct. 2018, Karlsruhe, Germany doi: 10.5194/isprs-annals-IV-1-61-2018, pp. 61-68, 2018.

[10] M. Madadikhaljan, R. Bahmanyar, S. Azimi, P. Reinartz, Peter and U. Sörgel, “Single-Image Dehazing on Aerial Imagery Using Convoultional Neural Networks”, in ISPRS International GeoSpatial Conference, 12.-14. Oct. 2019, Tehran, Iran, pp. 1-6, 2019.

[11] J. Han, J. Ding, N. Xue and G.-S. Xia, “ReDet: A rotation-equivariant detector for aerial object detection” in Proceedings of the IEEE/CVF Conference on Computer Vision and Pattern Recognition, pp. 2786–2795, 2021.

[12] S. Azimi, R. Bahmanyar, C. Henry and F. Kurz, “EAGLE: Large-scale Vehicle Detection Dataset in RealWorld Scenarios using Aerial Imagery”, in 2020 25th International Conference on Pattern Recognition (ICPR), ICPR 2020, 10.-15.01.2021, Milan/IT (virtual), pp. 6920-6927, 2021.

[13] A. Börner et. al., “Sensor Artificial Intelligence and its Application to Space Systems – A White Paper.”, 2020.